Pergamon

Int. J. Heat Mass Transfer. Vol. 41, No. 17, pp. 2705–2710, 1998

0017–9310/98 $19.00+0.00

PII: S0017–9310(97)00343–8

TECHNICAL NOTES

Effect of magnetic fields on oscillating mixed convection

BO PAN and BEN Q. LI†

School of Mechanical and Materials Engineering, Washington State University, Pullman, WA 99164-2920, U.S.A.

(*Received* 27 *June* 1997 *and in final form* 29 *October* 1997)

1. INTRODUCTION

Oscillating natural convection driven by g-jitter forces associated with microgravity and the magnetic field effect on the convection were discussed in an earlier paper [1]. In that paper, the mass flowrate is zero only for the case where the dimensionless temperature $r_T = -1$. This restriction can be eliminated by adding a pressure gradient so that the mass flowrate across the channel is zero for any arbitrary r_T. For a g-jitter driven flow in a cavity that bears direct relevance to crystal growth in space, the net mass flowrate in the system is zero. This system may be better modeled by considering flows in a long parallel plate channel with a pressure gradient, and this pressure gradient in reality comes from the end effects of the long parallel plate channel [2]. In some ground-based experiments intended for a fundamental understanding of magnetic field effects on g-jitter driven flows, an oscillating pressure gradient is applied in a channel to induce a flow, along with a transverse magnetic field [3–5]. This short technical note complements the earlier paper and discusses a general case of mixed convection driven by a combination of g-jitter and an oscillating pressure gradient under the influence of an applied magnetic field. Analyses of this type find applications in space fluid system design and interpreting the experimental measurements in microgravity flow and heat transfer systems [3–5].

2. ANALYSIS

Figure 1 shows the mixed convection problem under consideration. An electrically conducting fluid is at temperature T_0 and flows as a result of temperature and pressure gradients in between two parallel plates, infinitely long in both the x and z directions but at different temperatures. We consider here a fully developed, steady flow and thus the transverse velocity vanishes. Further we assume that the g-jitter field under consideration is spatially constant and otherwise varies with time harmonically and the flow at the entrance also oscillates because of an applied pressure gradient. The time varying gravity field will generate an oscillatory free convection velocity field. This is combined with the forced oscillating flow driven by a pressure gradient. If a transverse DC magnetic field is imposed as shown in Fig. 1, this oscillatory flow will be damped. The basic mathematical equations for this magnetically-affected fluid flow may be written below [1],

$$\frac{\partial u}{\partial t} = -\frac{1}{\rho}\frac{\partial p}{\partial x} + \nu\frac{\partial^2 u}{\partial y^2} + g(t)\beta_T(T-T_\infty) - \frac{\sigma}{\rho}(E_z + B_0 u)B_0. \tag{1}$$

For a time harmonic g-jitter component with a frequency ω, $g(t) = g_0 e^{j\omega t}$ and a similar oscillating pressure gradient, the flow field and the induced electric field should have a similar time varying behavior, provided that Re_m is small [1]. Hence, equation (1) can be re-written in a non-dimensionalized form,

$$\frac{\mathrm{d}^2 U}{\mathrm{d}Y^2} - \beta^2 U = Ha^2 E + \frac{\mathrm{d}P}{\mathrm{d}X} - \frac{Gr}{Re}\theta \tag{2}$$

where $\beta = \sqrt{Ha^2 + j\Omega}$ is a complex number.

For a fully developed channel flow, a linear temperature profile is attained [1, 5, 6],

$$\theta = (1-r_T)Y + r_T. \tag{3}$$

With equation (3) substituted into equation (2) and integrating with the no-slip boundary conditions,

$$U = 0 \quad \text{at} \quad Y = 0 \quad \text{and} \quad Y = 1$$

one has the solution for the velocity distribution across the channel,

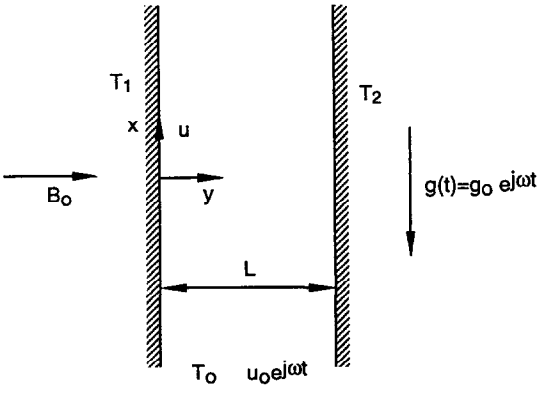

Fig. 1. Schematic representation of oscillating mixed convection problems and coordinate system used for calculations.

† Author to whom correspondence should be addressed. Tel.: 001 509 335 7386. Fax: 001 509 335 4662. E-mail: li@mme.wsu.edu.

NOMENCLATURE

B_0	applied magnetic field
E, E_z	nondimensionalized and dimensional electric field, $E = E_z/E_0$
E_0	electric field scale, $E_0 = B_0 u_0$
$g(t)$	g-jitter or residual gravity field
g_0	magnitude of g-jitter
Gr	Grashof number, $Gr = g_0\beta(T_2 - T_0)L^3/\nu^2$
Ha	Hartmann number, $Ha = LB_0\sqrt{\sigma/\nu\rho}$
I	total current
j	pure imaginary number, $j = \sqrt{-1}$
L	width of the channel
p	pressure
P	nondimensionalized pressure
r_T	nondimensionalized wall temperature parameter, $r_T = (T_1 - T_0)/(T_2 - T_0)$
Re	Reynolds number, $Re = u_0 L/\nu$
Re_m	magnetic Reynolds number, $Re_m = u_0 L\sigma\mu$
t	time
T, T_1, T_2, T_0	temperature, temperatures of wall 1, wall 2 and fluid
u	velocity
u_0	velocity scale
U	nondimensionalized velocity, a complex quantity
$\lvert U\rvert$	amplitude of velocity, $\lvert U\rvert = \sqrt{U \cdot U^*}$
$\hat{x}$	unit vector in the x-direction
$\hat{y}$	unit vector in the y-direction
y	y-coordinate
Y	nondimensionalized y coordinate, y/L.

Greek symbols

β	system parameter, $\beta = Ha^2 + j\Omega$
β_T	thermal expansion
δ_{Ha}	Hartmann layer thickness
θ	nondimensionalized temperature, $\theta = (T - T_0)/(T_2 - T_0)$
μ	magnetic permeability
ν	kinematic viscosity
ρ	density
σ	electrical conductivity
τ	nondimensionalized time, $\tau = t/\tau_0$
τ_0	time scale, $\tau_0 = L^2/\nu$
ω	applied frequency
Ω	nondimensionalized frequency, $\Omega = \omega L^2/\nu$.

Subscripts

T	temperature
x, y	x and y components of a vector field.

$$U = \frac{1}{\beta^2}\left[\left(Ha^2E + \frac{\partial P}{\partial X} - \frac{Gr}{Re}\right)\frac{\sinh(\beta Y)}{\sinh\beta} - Ha^2E - \frac{\partial P}{\partial X} + \frac{Gr}{Re}(r_T + (1 - r_T)Y) + \left(Ha^2E + \frac{\partial P}{\partial X} - \frac{Gr}{Re}r_T\right)\frac{\sinh(\beta(1 - Y))}{\sinh\beta}\right]. \quad (4)$$

The pressure gradient is determined by requiring that the flow satisfies the following condition,

$$\int_0^1 U(Y)\,dY = 1. \quad (5)$$

Thus, one has

$$\frac{\partial P}{\partial X} = -Ha^2E + \frac{1 + r_T}{2}\frac{Gr}{Re} + \frac{\beta^3\sinh\beta}{2\cosh\beta - \beta\sinh\beta - 2}. \quad (6)$$

For a system requiring the zero mass flow rate, the right hand of equation (5) should be zero and thus one can show that $\partial P/\partial X = -Ha^2E + (1 + r_T)/2$.

With the known velocity distribution, other relevant electromagnetic quantities such as induced electric field and total current in the channel can be calculated [1].

3. LIMITED BEHAVIOR

Some simple analyses may be readily carried out using the above equations. For a non-oscillating mixed convection under terrestrial condition without an applied magnetic field, a case that has been studied extensively in the literature [6, 7], the velocity profile given by equations (4) and (6) reduces to a familiar form [7],

$$U = \frac{Gr}{Re}(1 - r_T)\left(-\frac{Y^3}{6} + \frac{Y^2}{4} - \frac{Y}{12}\right) - 6Y^2 + 6Y. \quad (7)$$

This can be easily verified by letting $\beta \to 0$ and making use of the asymptotic relation $\sinh\beta = \beta + \frac{1}{6}\beta^3 + O(\beta^5)$.

For an oscillating mixed convection in the absence of an applied magnetic field, equations (4) and (6) are combined and then simplified by letting $Ha \to 0$, with the result,

$$U = \frac{1}{j\Omega}\left[\left(\frac{r_T - 1}{2}\frac{Gr}{Re} + \frac{(j\Omega)^{3/2}\sinh\sqrt{j\Omega}}{2\cosh\sqrt{j\Omega} - \sqrt{j\Omega}\sinh\sqrt{j\Omega} - 2}\right)\frac{\sinh(\sqrt{j\Omega}Y)}{\sinh\sqrt{j\Omega}} + \left(\frac{1 - r_T}{2}\frac{Gr}{Re} + \frac{(j\Omega)^{3/2}\sinh\sqrt{j\Omega}}{2\cosh\sqrt{j\Omega} - \sqrt{j\Omega}\sinh\sqrt{j\Omega} - 2}\right) \times \frac{\sinh(\sqrt{j\Omega}(1 - Y))}{\sinh\sqrt{j\Omega}} + (1 - r_T)\left(Y - \frac{1}{2}\right)\frac{Gr}{Re} - \frac{(j\Omega)^{3/2}\sinh\sqrt{j\Omega}}{2\cosh\sqrt{j\Omega} - \sqrt{j\Omega}\sinh\sqrt{j\Omega} - 2}\right]. \quad (8)$$

If the oscillation frequency is very large or $\Omega \gg 1$, the above equation becomes

$$U = \frac{\sqrt{j\Omega}}{\sqrt{j\Omega} - 2} - \left(\frac{\sqrt{j\Omega}}{\sqrt{j\Omega} - 2} + \frac{1 - r_T}{2}\frac{Gr}{Re\,j\Omega}\right)e^{-\sqrt{j\Omega}(1 - Y)} + \frac{Gr}{Re\,j\Omega}(1 - r_T)\left(Y - \frac{1}{2}\right) - \left(\frac{\sqrt{j\Omega}}{\sqrt{j\Omega} - 2} + \frac{1 - r_T}{2}\frac{Gr}{Re\,j\Omega}\right)e^{-\sqrt{j\Omega}Y}. \quad (9)$$

At the limit of $\Omega \to \infty$, we have

$$\lim_{\Omega\to\infty} U = 1 - e^{-\sqrt{j\Omega}Y} - e^{-\sqrt{j\Omega}(1 - Y)}. \quad (10)$$

From the above equation it is clear that a thin Stokes layer develops near the walls for high frequency oscillating flows, and the thickness of the layer is given by $\delta = (2/\Omega)^{1/2}$. This behavior has been observed in a flow induced by an oscillating solid boundary [8]. Similar results have also been obtained for oscillating free convection [1].

In the case of oscillating forced convection without an applied magnetic field and a temperature gradient, equation (8) may be further simplified as

$$U = \frac{\sqrt{j\Omega}(\sinh(\sqrt{j\Omega}Y) + \sinh(\sqrt{j\Omega}(1-Y)) - \sinh\sqrt{j\Omega})}{2\cosh(\sqrt{j\Omega}) - \sqrt{j\Omega}\sinh\sqrt{j\Omega} - 2}. \tag{11}$$

This is in contrast with the case where a magnetic field is present,

$$U = \frac{\beta(\sinh(\beta Y) - \sinh(\beta(Y-1)) - \sinh\beta)}{2\cosh\beta - \beta\sinh\beta - 2}. \tag{12}$$

The case for an oscillating mixed convective flow with a very large applied magnetic field may be obtained from equations (4) and (6) by letting $\beta \gg 1$. The result takes the same form as equation (8) but with β substituted for $\sqrt{j\Omega}$. At the limit of $\beta \to \infty$, one has

$$\lim_{|\beta|\to\infty} U = 1 - e^{-(1+j)Y/\delta_{Ha}} - e^{-(1+j)(1-Y)/\delta_{Ha}}.$$

Clearly a thin Hartmann layer arises near the vertical walls. The thickness of the layer is given by

$$\delta_{Ha} = \sqrt{\frac{2}{\sqrt{Ha^4 + \Omega^2} + Ha^2}}. \tag{13}$$

Thus, for magnetohydrodynamic oscillating mixed convective flows, the Hartmann layer near the walls depends on both the applied magnetic field and the oscillating frequency. The layer is thinner than either the Stokes layer for oscillating flows or the Hartmann layer for non-oscillating flows. The same conclusion has been obtained for natural convection driven by a g-jitter component of single frequency [1]. For a non-oscillating flow or $\Omega = 0$, δ_{Ha} defines the classical Hartmann layer thickness as discussed in the literature [9].

4. DISCUSSION

Figure 2 compares the oscillating mixed convection distributions across the width of the channel with and without an applied magnetic field over an oscillation period. In plotting the results, the conducting wall condition is applied. This will be true for all other results presented below. Non-conducting wall conditions can be studied following the same procedure as discussed in [1]. The quantity plotted along the vertical axis is $\mathrm{Imag}(U e^{j\Omega\tau}) = \mathrm{Real}(U)\sin(\Omega\tau) + \mathrm{Imag}(U)\cos(\Omega\tau)$, which represents the measurable value for a driving force $g = \mathrm{Imag}(g_0 e^{j\Omega\tau}) = g_0\sin(\omega t)$ and $u_0(t) = u_0\sin(\omega t)$. It is noticed that at around $\Omega\tau = \pi$ and $\Omega\tau = 2\pi$ the velocity profile also oscillates along the width of the channel but for the other times the velocity profile is approximately parabolic, as expected for symmetrically heated walls and for forced convection in a channel.

The velocity distribution in the channel for flows as a function of oscillating frequency is illustrated in Fig. 3. Clearly, the magnitude of the velocity decreases as the frequency increases. This is true even with an applied magnetic field, as long as the Hartmann number is small in comparison with the oscillation frequency. As the frequency goes higher or is predominantly bigger than the applied magnetic field, the flow resembles an oscillating Stokes flow in the vicinity

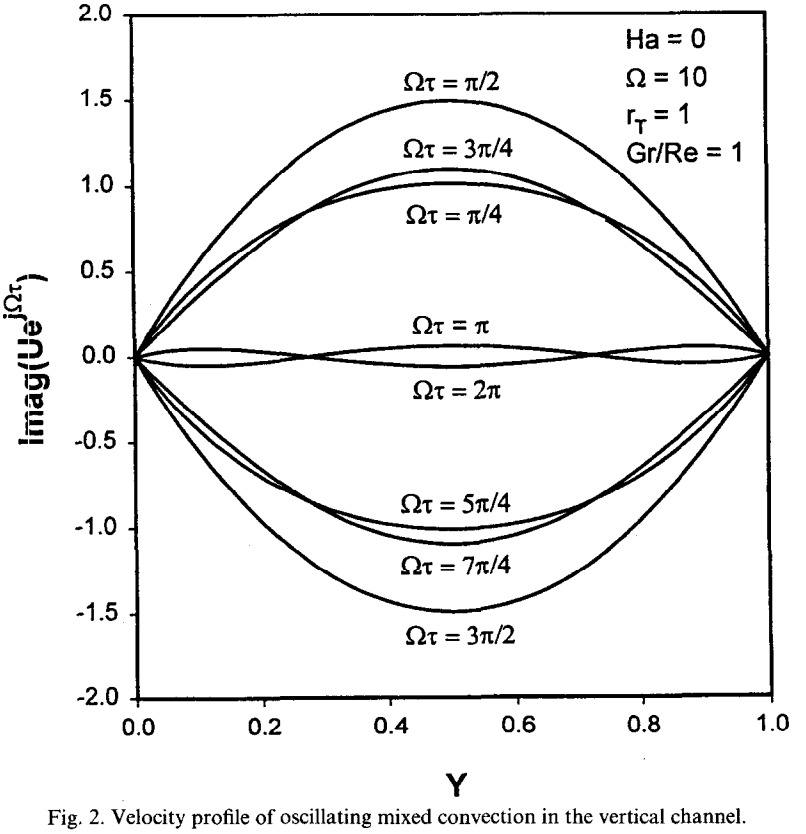

Fig. 2. Velocity profile of oscillating mixed convection in the vertical channel.

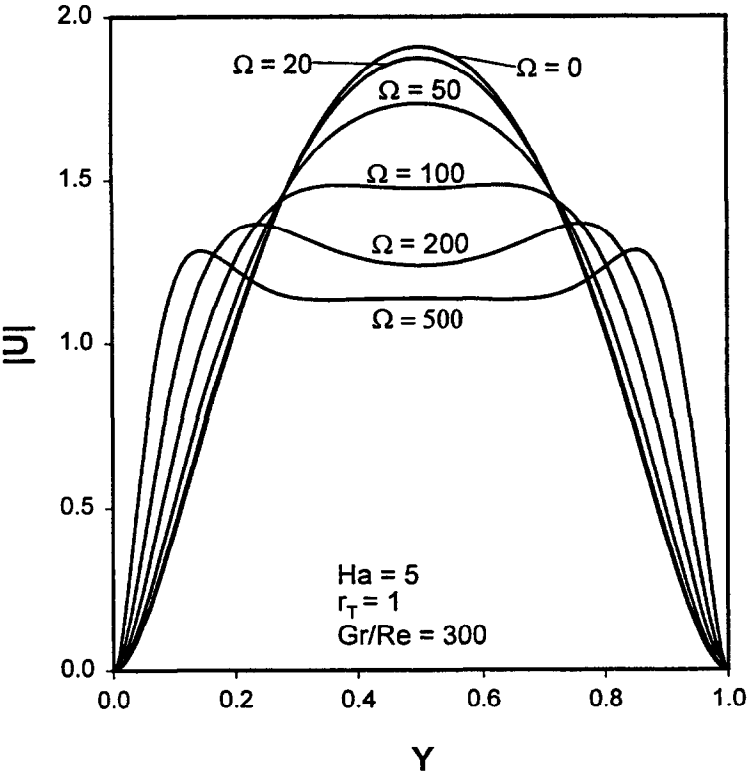

Fig. 3. Dependency of velocity distribution on oscillating frequency in the presence of an applied magnetic field.

of the solid walls [8]. As shown in the analyses above, this layer has an approximate thickness of $\delta = (2/\Omega)^{1/2}$, over which the flow velocity changes drastically and reaches a constant value.

The effect of an applied magnetic field on oscillating mixed convection is depicted in Fig. 4. It is seen that an increase in the applied magnetic field will help to reduce the fluid flow level. However, as the field strength increases, a thin Hartmann layer starts to develop near the solid walls. As shown above, the Hartmann layer for an oscillating flow depends on both the applied magnetic field and the oscillating frequency. This is the same for a g-jitter driven oscillating free convection with an applied field [1]. Comparison of Figs. 3 and 4 also indicates the difference between the effect of high frequency and that of a large magnetic field on the flow. There exists a hump near the wall that overshoots the asymptotic value for a high frequency convective flow (see Fig. 3), while such a hump does not show up with a high magnetic field (see Fig. 4). This difference is explained by the fact that for a high frequency flow the velocity change near the walls is determined by $e^{-(1+j)Y\sqrt{\Omega/2}}$, while the magnetic damping occurs by e^{-HaY}. It is remarked here that the frequency effect on an oscillating flow resembles closely the decaying behavior of a high frequency electromagnetic wave within a highly conducting surface [9].

The streamwise velocity profile with a moderate magnetic strength ($Ha = 5$) is calculated using equations (4) and (6) and is plotted in Fig. 5 for $r_T = 0$, 0.3 and 0.6. Note that the velocity profile for $r_T = 1$ is the same as for $Gr/Re = 0$ [see equation (4)]. As seen from the figure, the velocity profile is skewed with an increase in Gr/Re. This is similar to the results reported by Aung and Worku [7]. However, in comparison with their results (see Fig. 1 in [6]), the presence of a magnetic field reduces the magnitude of the streamwise velocity, as expected. Also, the point at which the flow at the cold wall ($Y = 0$) reverses it direction becomes smaller with an applied field. For example, at $Gr/Re = 500$ and $r_T = 0.3$, the flow reversal starts at $Y = 0.5$ without a magnetic field [7], whereas with a Hartmann number of five, the flow reversal point is at $Y = 0.3$ (see Fig. 5).

It is noteworthy that in the last two figures, the velocity profile plotted is for $\Omega\tau = \pi/2$, which corresponds to Imag$(Ue^{i\Omega\tau})$ = Real(U). For a different $\Omega\tau$ value, the asymptotic velocity can be different from one and its value is determined by Imag$(Ue^{i\Omega\tau}) = \sin\Omega\tau$. This is different from the magnetic damping of non-oscillating mixed convection.

5. CONCLUSIONS

Theoretical analyses of oscillating mixed convection have been presented for parallel-plate channels. As for the non-oscillating flow case, flow reversal occurs as well for oscillating flows. The application of a magnetic field helps to reduce the flow velocity level and also moves the flow reversal point closer to the cold wall. Analyses show that a Stokes layer exists near the solid walls for oscillating flows. Also, a thin Hartmann layer exists near the solid boundaries for oscillating mixed convection in the presence of an applied magnetic field. The thickness of the layer depends on both the applied magnetic field and the oscillating frequency, as for the case of oscillating free convection.

Acknowledgement—The authors gratefully acknowledge support of this work by NASA, Grant no. NCC8-92.

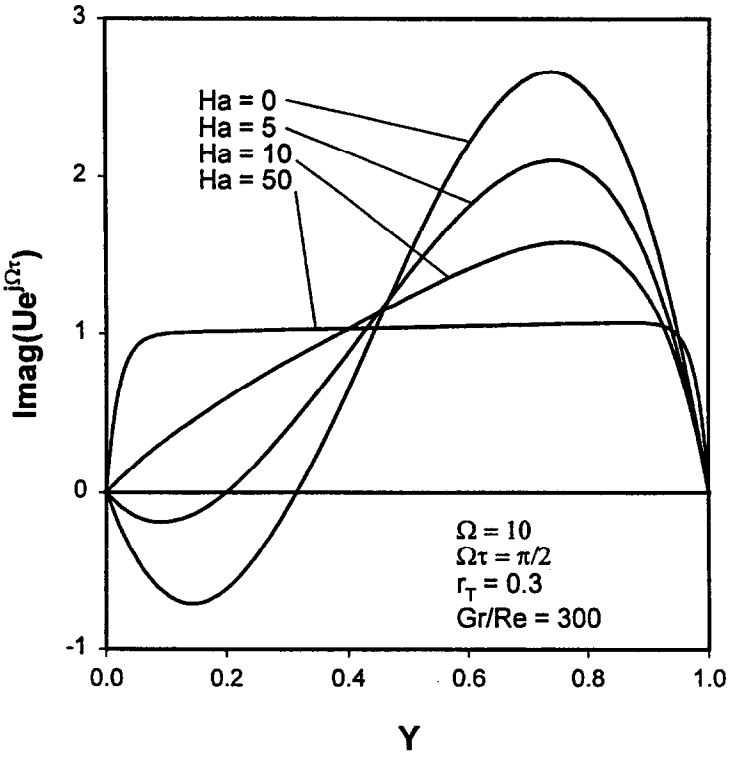

Fig. 4. Magnetic damping effect on oscillating mixed convection in the vertical channel.

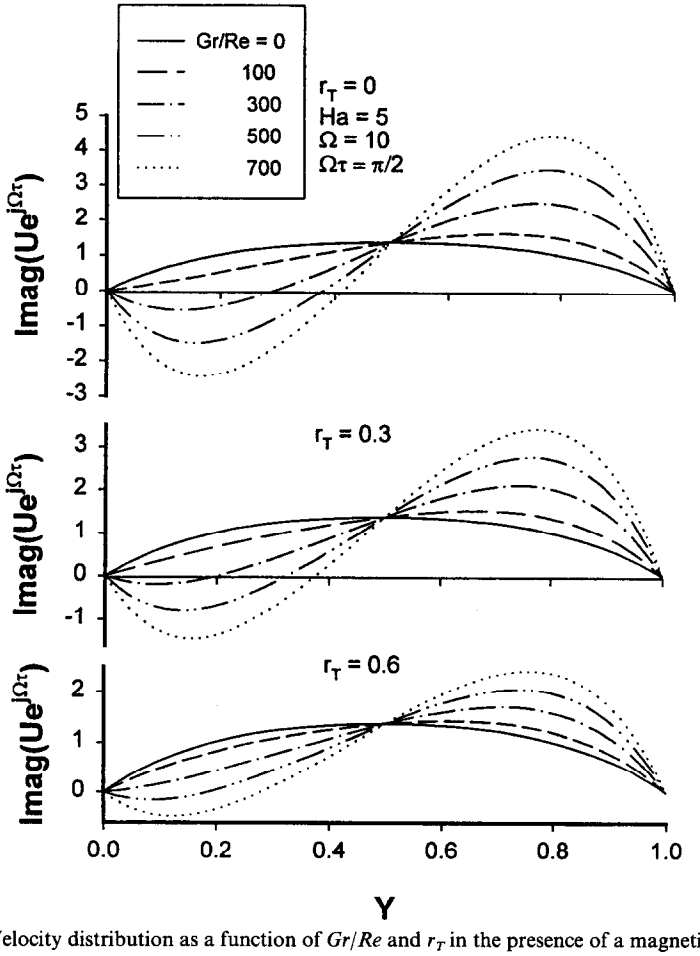

Fig. 5. Velocity distribution as a function of Gr/Re and r_T in the presence of a magnetic field.

REFERENCES

1. Li, B. Q., *g*-jitter induced free convection in a transverse magnetic field. *International Journal of Heat and Mass Transfer*, 1996, **39**(14), 2853–2860.
2. Bejan, A., *Heat Transfer*, Chap. 7. John Wiley and Sons, New York, NY, 1992.
3. Lehoczky, S., Szofran, F. R. and Gillies, D. C., Growth of solid solution single crystals. Second United States Microgravity Payload, Six Month Sciences Report, NASA MSC, 1994.
4. Antar, B. N. and Nuotio-Antar, V. S., *Fundamentals of Low Gravity Fluid Dynamics and Heat Transfer*. CRC Press, Boca Raton, FL, 1993.
5. Nelson, E. S., An examination of anticipated *g*-jitter on space station and its effects on materials processes. NASA TM 103 775, 1991.
6. Aung, W., Fully developed laminar convection between vertical plates heated asymmetrically. *International Journal of Heat and Mass Transfer*, 1972, **15**, 577–1580.
7. Aung, W. and Worku, G., Theory of fully developed, combined convection including flow reversal. *Journal of Heat Transfer*, 1986, **108**, 485–488.
8. Panton, R. L., *Incompressible Flow*. Chap. 11. John Wiley and Sons, New York, NY, 1984.
9. Jackson, J. D., *Classical Electrodynamics*. Chap. 10. John Wiley and Sons, New York, NY, 1976.

Pergamon

Int. J. Heat Mass Transfer. Vol. 41, No. 17, pp. 2710–2713, 1998

0017–9310/98 $19.00+0.00

PII: S0017–9310(97)00329–3

Experimental study on the relation between thermophoresis and size of aerosol particles

AKIRA TODA,† HISATAKA OHNISHI, RITSU DOBASHI and TOSHISUKE HIRANO

Department of Chemical System Engineering, Faculty of Engineering, The University of Tokyo, 7-3-1 Hongo, Bunkyo-ku, Tokyo 113, Japan

and

TAKASHI SAKURAYA

Japan Space Utilization Promotion Center, 3-30-16 Nishiwaseda, Shinjuku-ku, Tokyo 169, Japan

(*Received* 9 *May* 1997 *and in final form* 24 *October* 1997)

1. INTRODUCTION

In a field with temperature gradient, it is known that mass-transfer is also induced by the temperature gradient. When a small particle is suspended in such a field, it will be driven to move toward a colder region. This phenomenon is known as thermophoresis. The study on thermophoresis, which was started at the beginning of this century, has been performed actively by many researchers because of its practical importance [1–4] and theoretical interest [5–8].

In order to elucidate the thermophoretic effect, the basic data are indispensable. However, the measurement of the thermophoretic effect is not so easy. Small particles may be easily moved by various kinds of effects. Distinguishing only the thermophoretic effect from other effects quantitatively needs a rather complicated process which is likely to cause errors. Therefore, in order to get reliable data, it is desirable to perform careful experiments in simple fields where other effects are negligible.

In normal gravity, however, we can hardly eliminate the effects of gravity and natural convection. The gravitational effect changes with the diameter and/or density of the particles and prevents us from simplifying the experiment. Especially, the gravitational effect on large and heavy particles exceeds the relatively small thermophoretic effect and makes the accurate measurement difficult.

The effect of natural convection is a more serious problem in the measurement. The effects of natural convection and thermophoresis are induced simultaneously by the same temperature gradient, and determining them separately and quantitatively by the experiments is quite difficult. It has been the main issue of the experimental studies how the effect of natural convection should be estimated. Because of the reason described above, accumulation of data in the past has been not enough to verify various theoretical results or to predict accurately the behavior of particles.

We successfully avoided these difficulties by establishing an experimental method utilizing microgravity environment, where the effects of gravity and natural convection became negligible [9]. It was found that our experimental method and microgravity environment gave us ideal fields for the measurement. The experimental fields were found to be quasi-steady with monotonous temperature gradient, and the movement of individual particles induced only by the thermophoretic effect could be observed. By performing experiments in microgravity, we are now able to determine the temperature gradient and the corresponding particle vel-

† Author to whom correspondence should be addressed.